

RESEARCH

Open Access



Phenotypes and cytokines of NK cells in triple-negative breast cancer resistant to checkpoint blockade immunotherapy

Youlong Wang^{1†}, Yongluo Jiang^{2,3†}, Fadian Ding^{4,5,6,7†}, Jun Lu⁸, Tong Huang⁹, Guanqing Zhong^{3,10*}, Pengfei Zhu¹¹, Yue Ma¹², Jin Li¹³, Xinjia Wang^{14,15}, Jiakai Lin¹⁶, Hongjun Zheng¹⁷, Weidong Wang¹⁵, Yiwei Xu¹⁸, Xiajie Lyu¹⁹, Yu Si Niu²⁰, Xin Qi²¹, Jinjian Li⁸, Bocen Chen²², Tingting He²³, Jiling Zeng^{2,3} and Yifei Ma^{4,5,6,7*}

Abstract

Neoadjuvant checkpoint blockade immunotherapy (NATI) significantly prolonged outcomes for triple-negative breast cancer (TNBC). Residual tumor cells that survive NATI represent high-risk cell populations with metastatic potential and usually evade immunosurveillance by NK cells. Using an 82-protein panel, we here profiled single-cell membrane proteomics of CD56+ (NCAM1+) NK cells from tumor, peri-cancerous tissue, as well as peripheral blood from 28 TNBC patients post-NATI of residual cancer burden II/III. Unsupervised clustering resulted in several distinct clusters: 2 tumor-infiltrating NK (TINK) clusters with divergent functions of immune activation (TNFRSF7+) and suppression (SELL+); 2 immuno-suppressive peri-cancerous clusters; and 1 periphery-specific cluster. Considering the contradiction of the 2 TINK clusters, we further tested cytokine functions of SELL+ and TNFRSF7+ TINKs by single-cell secreting proteomics using a 32-cytokine panel. Consistently, SELL+TINK clusters were characterized by immuno-suppressive secretion patterns (IL10+). A low proportion of SELL+TINK cluster and low proportion of IL10+ secreting SELL+TINK cluster (single-cell secreting proteomics) were both associated with better progression-free survival time. These findings were validated in an independent cohort of 15 patients during 16-month follow-up. Overall, we identified a distinct immuno-suppressive TINK cell group, featuring IL10+ secreting and SELL expression with a strong relation to poor survival prognosis in TNBC patients post-NATI.

Introduction

Triple-negative breast cancers (TNBC) lack expression of HER2, ER, and PR, have a high risk of metastasis, and bring about poor survival prognosis, accounting for 10–15% of invasive breast cancers [1]. Neoadjuvant therapy by immune checkpoint inhibitors (NATI) is reported as a preferred regimen for early-phase TNBC due to high probability of achieving better resection rates which can substantially increase pathological complete response (pCR) and prolong survival outcomes [2, 3]. Mechanism of augmented anti-tumor immunity in immune checkpoint inhibition (ICI) relates to progression death-1 (PD1) receptor or ligand (PDL1) blockage and

[†]Youlong Wang, Yongluo Jiang and Fadian Ding contributed equally to this work.

*Correspondence:
Guanqing Zhong
zhongggq@sysucc.org.cn
Yifei Ma
myf61872169@163.com

Full list of author information is available at the end of the article



enhanced T effector cell functions [4]. However, clinical trial outcomes related to NATI exhibited that a number of patients could not reach pCR endpoints, suggesting relatively high proportions of residual tumor cells post NATI [5]. These treatment-resistant cells were clinically relevant for high residual cancer burden (RCB), which has been associated with poor long-term survival [6]. Residual cancer cells that survive NATI may come from those populations with intrinsic resistance to NATI with such potential as future metastasis and recurrence [4]. In addition to inherent NATI resistance of tumor biology, treatment-resistant cancer cells may exploit microenvironment for cytotoxicity evasion. The microenvironment of early-phase TNBC resistant to NATI has not been fully understood, particularly for those with high RCB. Thus, a profiling investigation of immune cells associated with high RCB may unveil potential cellular targets of resistance to NATI.

Effector immune cells are key elements for antitumor immunity, which are comprised mainly of cytotoxic CD8+ T cells and NK cells [7, 8]. CD8+ T cells require MHC I coordinating with antigen epitope and other activating signals to initiate adaptive immunity and tumor cell attack. Following PD-1 blockade, T-cell activation causes killing of tumor cells abundant in membrane

antigen epitopes [8]. Unfortunately, a large proportion of tumor cells undergo immune adaptive editing to conceal MHC-I-related tumor antigens to evade adaptive immune response [9]. However, NK cells, as MHC-independent effectors, may complement T cell function for antitumor immunity by killing tumor cells with shrouded antigen epitopes [9]. Also, NK cells were associated with significant functions of immune modulation which is largely unknown.

Importantly, immune microenvironment phenotype analysis from resected TNBC specimens suggested low-level infiltrating CD3+ lymphocytes and poor immunogenic response, enhancing the importance of antigen-free recognition mechanism by NK cells [10]. Further, immune modulating functions of NK cells need further investigation. Currently, little is known about NK cell components or functions in the immune microenvironment following NATI. Further, NK cells from pericancerous tissues as well as from peripheral circulation may serve as critical reservoirs of cytotoxicity, of which phenotypes or functions have not been fully characterized so far. Thus, a deep study of NK cell subset may reveal potential cellular targets to overcome resistance happening in the immune microenvironment.

Results

Patient sample characteristics and NK cell clustering

By means of single-cell membrane proteomics, we evaluated CD56+ (NCAM1+) NK cells in paired samples of human TNBC post-NATI treatment from 28 patients. Mean age was 39.29 ± 5.94 years, and most patients were receiving PD-1 blockers ($n=22$) as NATI before surgery (Table 1). NK cells were procured from histologically confirmed tumor (T), adjacent breast tissue (peri-cancerous tissue, AT), and peripheral blood mononuclear cells (PBMC). These paired samples underwent single-cell preprocessing as well as isolation for experiment, which finally yielded 54,655 NK cells in total, including 20,207 cells from T, 18,298 cells from AT, and 16,150 cells from PBMC. By means of unbiased clustering in *Seurat* packages, we grouped these cells into 11 clusters (c0~c10) visualized as UMAP plot (Fig. 1A), with the largest cluster containing 13,462 cells and the smallest cluster containing 1196 cells. All cell clusters expressed low levels of CD56 (NCAM1, Fig. 1D, Supplementary Fig. 1A). Chi-square tests were performed to compare between specimen groups and clusters (Fig. 1B-C) and striking discrepancy was found for cell distributions. Cluster 2 and 5 predominately represented NK cells from T (>80% cells). Cluster 9 as well as 10 were mainly from AT, whereas cluster 3 came mainly from the PBMC. Other clusters were not differential among the three specimen groups. These findings preliminarily suggested different subclusters of cells defined by diverse compositions

Table 1 Clinical data from the breast cancer patient

	Mean/count	std/%
Age	39.29	5.94
Follow_up_month	12.93	3.88
Outcomes		
Disease progression	20	71.43%
Stable disease	8	28.57%
RCB_score		
II	13	46.43%
III	15	53.57%
Grade before NATI		
2	15	53.57%
3	13	46.43%
Clinical stage before NATI		
2	9	32.14%
3	19	67.86%
Tumor stage before NATI		
2	8	28.57%
3	10	35.71%
4	10	35.71%
Node stage before NATI		
1	14	50.00%
2	7	25.00%
3	7	25.00%
ICI types		
PD_L1 blockers	6	21.43%
PD1 blockers	22	78.57%

RCB_score, residual cancer burden score. ICI types, immune checkpoint inhibitor types

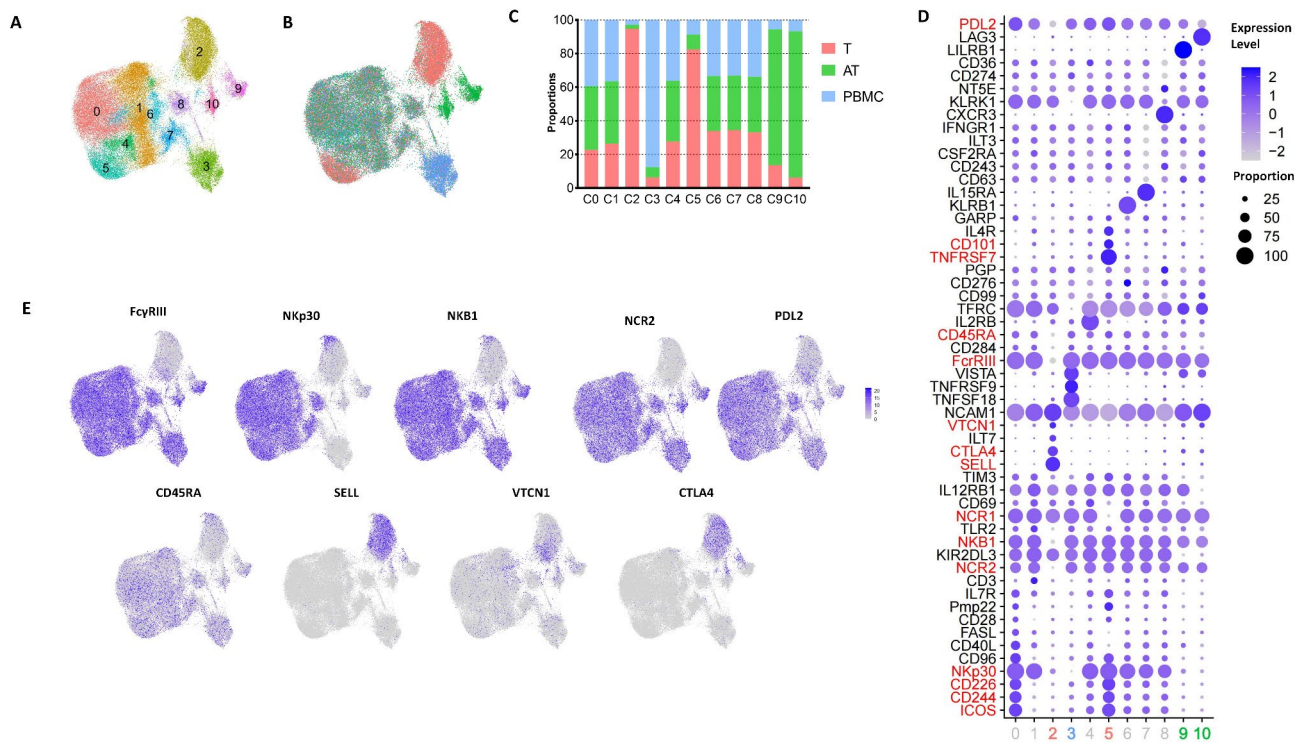


Fig. 1 Single-cell membrane proteomics-defined auto-clustering of NK cells in TNBC patients. **A.** Membrane proteomics-defined UMAP plot visualizing NK cell clusters from tumor, peri-cancerous, and periphery specimen. **B.** Membrane proteomics-defined UMAP plot visualizing NK cells grouped by specimen. **C.** Bar plot showing cell proportions of specimen group in each proteomics-defined NK clusters. **D.** Dot plot showing expression levels and cell proportions in each cluster, with red marks identifying NK cell-specific markers. NCAM1 (CD56) expression across clusters in tumor (T), adjacent tissue (AT), and peripheral blood (PBMC). **E.** UMAP plot visualizing expression of featured membrane markers in cluster 2 (related to supplementary Fig. 1)

of NK membrane markers in specimens from T, AT, and PBMC of TNBC patients.

Cancer-specific NK cells from tumor, peri-cancerous, and periphery exhibited mainly immuno-suppressive phenotypes

We first examined feature markers of tumor-infiltrating NK cells (TINK, Fig. 1D-E, Supplementary Fig. 1A) defined by single-cell membrane proteomics. We found cluster 2, which is a large cluster, has relatively low expression of FcγRIII (CD16) compared to other clusters, and thus lacks typical function of antibody-dependent cellular cytotoxicity. NK cell-specific receptors of NCR2 and NKp30 were also low-expressed in this cluster, indicating a hypofunctional NK subset. In addition, this cluster lacks important NK cell immune regulators, including mainly NKB1, PDL2, and CD45RA (PTPRC). Highly expressed membrane proteins in this cluster included SELL (CD62L), indicating cell adhesion functions, and VTCN1 and CTLA4, indicating immune inhibitory signature. Overall, cluster 2 of TINK exhibited functionally deficient phenotypes.

Another cluster specific to TINK, cluster 5, however, exhibited high levels of markers relevant to cellular activation, including TNFRSF7 (CD27) and CD101 (Fig. 1D,

Supplementary Fig. 1B, D). These cells shared several activating markers with cluster 0, including CD226, CD244, and ICOS. Also, this cluster expressed several NK-specific receptors not found in cluster 2, including FcγRIII, NKp30, and NKB1, although NCR1 was poorly found in this cluster. Overall, cluster 5 exhibited a high level of immune activation which is different from cluster 2.

Clusters specific to peri-cancerous specimens, including cluster 9 and 10, expressed high levels of immuno-suppressive feature markers, including LILRB1 (cluster 9) and LAG3 (cluster 10), with a shared expression of VISTA in both clusters (Fig. 1D, Supplementary Fig. 1C, D). Functional NK receptors were deficient in both clusters, including KIR2DL3 and NKp30, suggesting function deficiency in NK cells of peri-cancerous specimens. In addition, expression of IL12RB1 was found in all other clusters but was lacking in cluster 10. Overall, cluster 9 and 10 were phenotypically similar with high levels of immunosuppressive marker expression.

Cluster 3, which is specific to the periphery of TNBC patients, was characterized by a mixed function of both immune suppression and activation (Fig. 1D, Supplementary Fig. 1C, D). Expression of TNFRSF9, which is a feature marker of this cluster, suggested activating the

potential of these cells. High levels of immuno-suppressive markers were found in this cluster, such as VISTA and TNFRSF18 (GITR), suggesting immune suppression potential in NC cells from the periphery. This cluster also featured low expression of KLRK1, suggesting functional deficiency. Finally, based upon published information and dataset we annotated these clusters by feature protein antibodies calculated with expression levels (Supplementary Fig. 2).

Divergent secreting cytokines of tumor-infiltrating NK cell subclusters

Considering immunophenotypes of disease-specific TINK cells were identified as contradictory in SELL + NK, which is immuno-inhibitory, and in TNFRSF7 + NK, which is excitatory, we then tried to investigate the specific secreting cytokines of these 2 subsets. As such, SELL and TNFRSF7 microbeads were employed to positively sort cells, and these sorted cells underwent single-cell secreting proteomics in a commercial 32-protein chip. We finally obtained 12,417 cells, including 6483 SELL + NK cells and 5934 TNFRSF7 + NK cells from these patients for unbiased clustering.

By means of *Seurat* packages, we grouped these cells into 9 clusters (c0~c8) visualized as UMAP plot (Fig. 2A), which were annotated by feature protein

antibodies calculated with expression levels, with the largest cluster containing 2842 cells and the smallest cluster containing 1196 cells. Striking discrepancy was found for cell cluster, cell count, and grouping, indicating functional discrepancy of SELL + NK and TNFRSF7 + NK cells (Fig. 2B). Specifically, cluster 2, 4, and 7 were mainly from the secretome of SELL + NK cells, whereas cluster 5, 6, and 8 came mainly from the secretome of TNFRSF7 + NK cells (Fig. 2C). Other clusters were not group-specific (cluster 0,1, and 3). We then annotated these clusters by the highest-secreting protein. We found that cluster 2, 4, and 7 were featured by high levels of immuno-suppressive cytokines, including IL4, IL10, and TGF β 1, suggesting that secretome of SELL + NK cells were associated immuno-suppression activity in tumor microenvironment. Cluster 5 and 6 featured high levels of immuno-activating cytokines, including IL7, suggesting that the secretome of TNFRSF7 + NK cells were activating other immune cells. Interestingly, we identified that cluster 8 was a multi-functional cell that co-secreted 5 types of effecting cytokines, including GZMB, IFNG, TNFA, PRF1, and CCL3 (Fig. 2D).

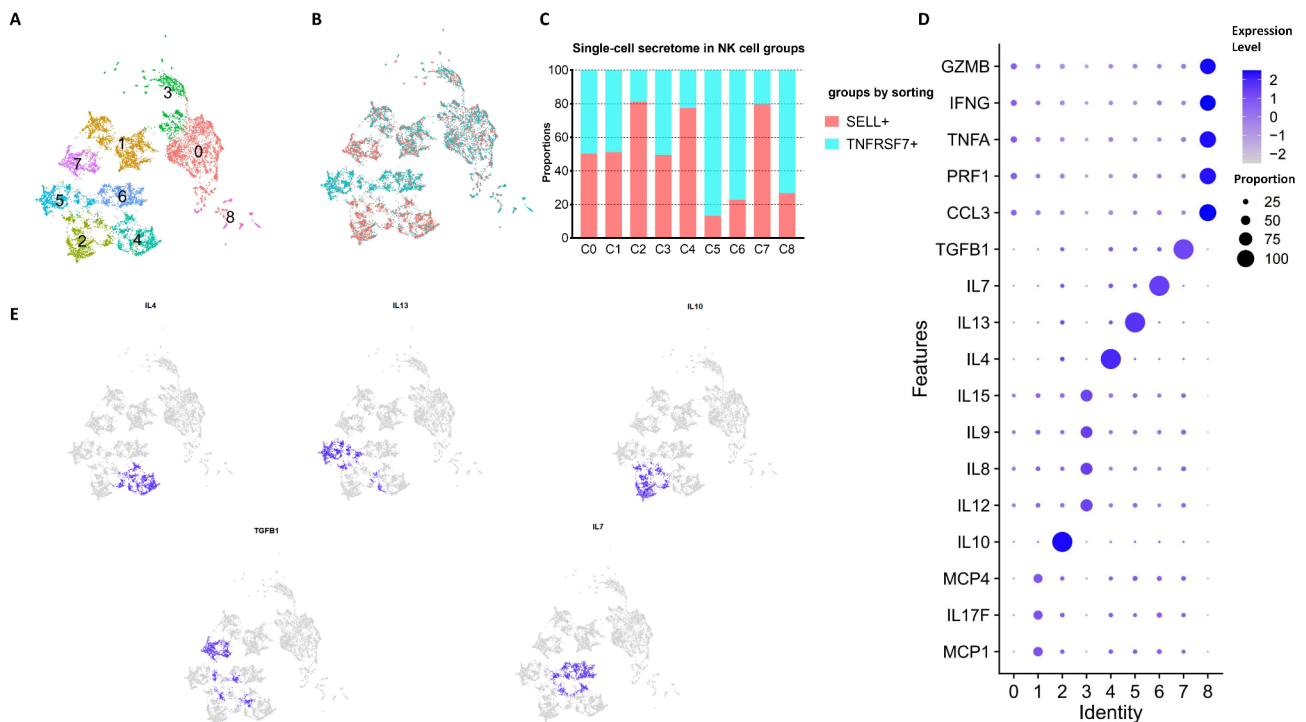


Fig. 2 Single-cell secreting proteomics-defined auto-clustering of tumor-infiltrating SELL+ and TNFRSF7+ NK cells in TNBC patients. **A.** Single-cell secreting proteomics-defined UMAP plot visualizing secreting tumor infiltrating SELL+ and TNFRSF7+ NK cell clusters. **B.** Single-cell secreting proteomics-defined UMAP plot visualizing cells grouped by specimen (SELL+ sorted and TNFRSF7+ sorted cells). **C.** Bar plot showing cell proportions of specimen group in each cluster. **D.** Dot plot showing single-cell cytokine levels and cytokine-secreting cell proportions in each cluster. **E.** UMAP plot visualizing expression of featured cytokines in each cluster

Tumor-infiltrating IL10-secreting SELL+ NK cell is independently associated with poor survival prognosis in both development and validation cohort

To this end, we illustrated the immunophenotypes of NK cells in the peripheral blood, peri-cancerous, and tumor tissues, in which tumor tissue featured primarily inhibitory phenotypes in membrane proteins and cytokine patterns. Prior research suggested that such inhibitory NK phenotypes were associated with poor response to checkpoint blockade therapy [11, 12], but to which extent these microenvironments were associated with patient prognosis has not been reported. Here, we made an association analysis of our findings with the progression-free survival (PFS) time of patients from development and validation cohort (see demographics of validation cohort in Table 2) to illustrate the clinical implications of single-cell clustering.

Overall, these 28 patients from development cohort were followed up for 18 months, with 20 patients (71.4%) reaching the endpoint of progression and 8 patients not progressing during follow-up. As either single-cell secreting proteomics or membrane proteomics was unbiased in each cluster, we first made a binary classification of proportions of clusters and did univariate association

analysis of these cluster proportions as well as clinicopathological data with PFS in survival analysis (Fig. 3A-C). We found that, in single-cell membrane proteomics, cluster 2 proportion was the only cluster associated with PFS (Fig. 3A). Specifically, lower proportions of cluster 2 were associated with better PFS (median time of PFS: 18 months versus 12 months, Fig. 3D). This finding was further validated in multivariate COX proportional models in which clinicopathological data were set as covariates (HR=0.26, Fig. 3E). Combined with prior findings, this result suggested that inhibitory membrane phenotype was associated with poor patient prognosis.

We then made a similar analysis in single-cell secreting cell clusters in SELL+ and TNFRSF7+ sorted NK cells in tumor tissues. We found that cluster 2 (featured by secreting IL10 cytokine) proportion was associated with PFS prognosis (Fig. 3B). A lower proportion of cluster 2 in secreting proteomics was associated with better PFS in univariate and multivariate survival analysis (Fig. 3F-G). These findings were further verified in validation cohort of single-cell proteomic analysis and subsequent 16-month follow-up in 15 patients (Supplementary Fig. 3-4). Our finding overall highlighted that the inhibitory immune environment, illustrated as both membrane phenotype and secreting cytokines at single-cell level, was associated with poor survival prognosis in TNBC patients (Fig. 4).

Table 2 Clinical data in validation cohort

	Mean/count	std/%
Age	55.40	7.99
Follow up (month)	10.60	3.93
Outcomes		
Disease progression	8	53.33%
Stable disease	7	46.67%
RCB score		
II	8	53.33%
III	7	46.67%
Grade before NATI		
2	7	46.67%
3	8	53.33%
Clinical stage before NATI		
2	8	53.33%
3	7	46.67%
Tumor stage before NATI		
1	1	6.67%
2	6	40.00%
3	5	33.33%
4	3	20.00%
Node stage before NATI		
1	7	46.67%
2	5	33.33%
3	3	20.00%
ICI types		
PD_L1 blockers	5	33.33%
PD1 blockers	10	66.67%

RCB_score, residual cancer burden score. ICI types, immune checkpoint inhibitor types

Discussion

By means of single-cell membranous as well as secreting proteomic experiments, we mainly profiled membrane markers and secreting cytokines of NK cell subsets in tumoral tissue, peritumoral tissues, and peripheral blood samples of high-risk TNBC patients after neoadjuvant checkpoint blockade. Importantly, we identified a tumor-infiltrating IL10-secreting SELL+ NK cell subset, as an immuno-inhibitory player in tumor microenvironment, which was associated with poor survival prognosis during an 18-month follow-up, which was further validated in an independent clinical cohort. This finding corroborated previous research hypothesis that cytotoxic cell functionally deficiency and inhibitory immuno-environment may strongly affect immunotherapy outcomes [13], and further pointed out specific functions of NK cell subsets with a relatively large sample size. Considering the immunologically “cold” NK cell may relate to cell survival and metastasis of treatment-resistant cancer cells in TNBC residual lesions [4], our preliminary landscape of NK cell phenotype may shed light on future research insights.

Research suggested that breast cancer cells evade NK-mediated anti-tumor activity through down-regulating NK cytotoxicity [14], resulting partially into functionally as well as phenotypically naive NK cells. Consistently, we

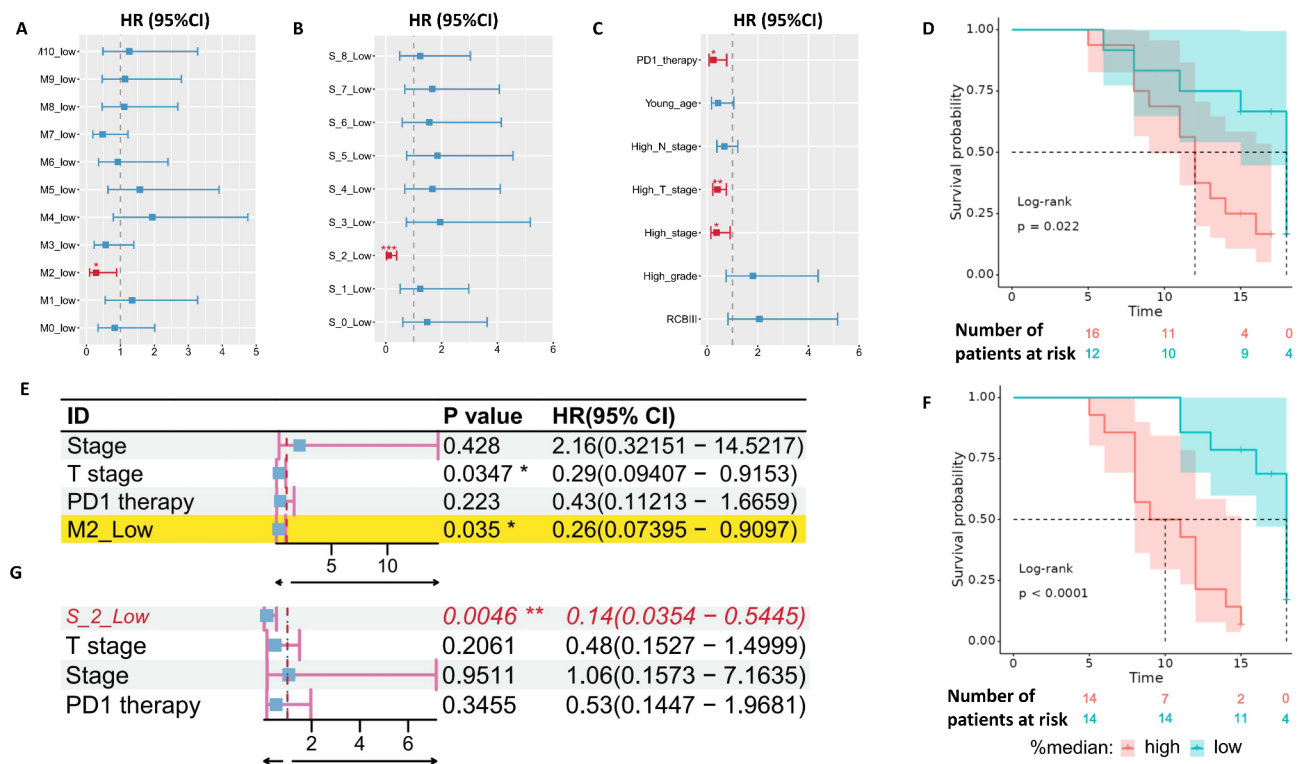


Fig. 3 Survival analysis associated with single-cell membrane and secreting proteomics. **A.** Univariate survival analysis (Cox proportional hazards model) showing hazards ratio (HR) and 95% confidence interval (95%CI) of progression-free survival (PFS) time in 18-month follow-up, associated with single-cell membrane proteomics-defined cluster proportion (%) in each patient, with M0_low to M10_low indicating low %each cluster (e.g. M0_low indicates lower %cluster 0). **B.** Univariate survival analysis showing HR and 95% CI of PFS time, associated with single-cell secreting proteomics-defined cluster proportion in each patient, with S₀_low to S₈_low indicating low %each cluster (e.g. S₀_low indicates lower %cluster 0). **C.** Univariate survival analysis (Cox proportional hazards model) showing HR and 95% CI of clinicopathological covariates. **D.** Kaplan-Meier Survival curve stratified by median patient proportions of single-cell membrane proteomics-defined cluster 2 (M2). **E.** Multivariate survival analysis (Cox proportional hazards model) showing HR and 95% CI of PFS time, testing M2_Low% as an independent variate adjusting for clinicopathological covariates. **F.** Kaplan-Meier Survival curve stratified by patient median proportions of single-cell secreting proteomics-defined cluster 2 (S₂). **G.** Multivariate survival analysis showing HR and 95% CI of PFS time (18-month follow-up), testing S₂_Low% as an independent variate adjusting for clinicopathological covariates

found that NK cells specific to tumor specimen (cluster 2) lacked expression of many classic markers of NK cell functions, such as NKB1, NCR2, and NKp30, suggesting an immuno-inhibitory role of such NK cluster [4]. However, according to single-cell transcriptomic research findings in previous research, featured protein in membrane proteomics of these NK cell clusters exhibited substantially different levels of expression, indicating high levels of phenotypic heterogeneity in NK cells [4, 13, 15]. Similarly, we found that functionally activated NK cell was present inside tumor specimen with differentially high levels of many functional markers (cluster 5), suggesting immune activation state of such cluster.

Notably, membrane profiling of NK cells from different specimen sites in these 28 TNBC patients gave us an opportunity to subclassify NK cells into multiple cell clusters at protein expression and cytokine secretion levels in different sites. These cells were clustered and compared at specimen level to yield specimen-specific and common NK cells, in which two functionally divergent

cell clusters, SELL+ and TNFRSF7 + TINK cells, were identified to be of prognostic value. SELL+ NK cells may play critical role in migration to tumor environment but their functions may be inhibited by inhibitory cytokines within tumor microenvironment [16]. TNFRSF7 may thus salvage the inhibited functions by creating accelerator functions for anti-cancer immunity and may be potential target for cancer immunotherapy [17]. This is why we designed another experiment in which secreting functions of two types of NK cell subtypes, and did correlative analysis with patient outcomes during 18-month follow-up.

Our findings suggested that high levels of IL10-secreting SELL+ NK cells were associated with poor outcomes, indicating inhibitory functions within tumor microenvironment. IL10 is a key immuno-inhibitory cytokine in normal tissues to prevent autoimmunity by inhibiting activity of T cells and NK cells [18]. In tumor microenvironment IL10 thus represent one of the most strong inhibitory cytokines against immunotherapy [18, 19].

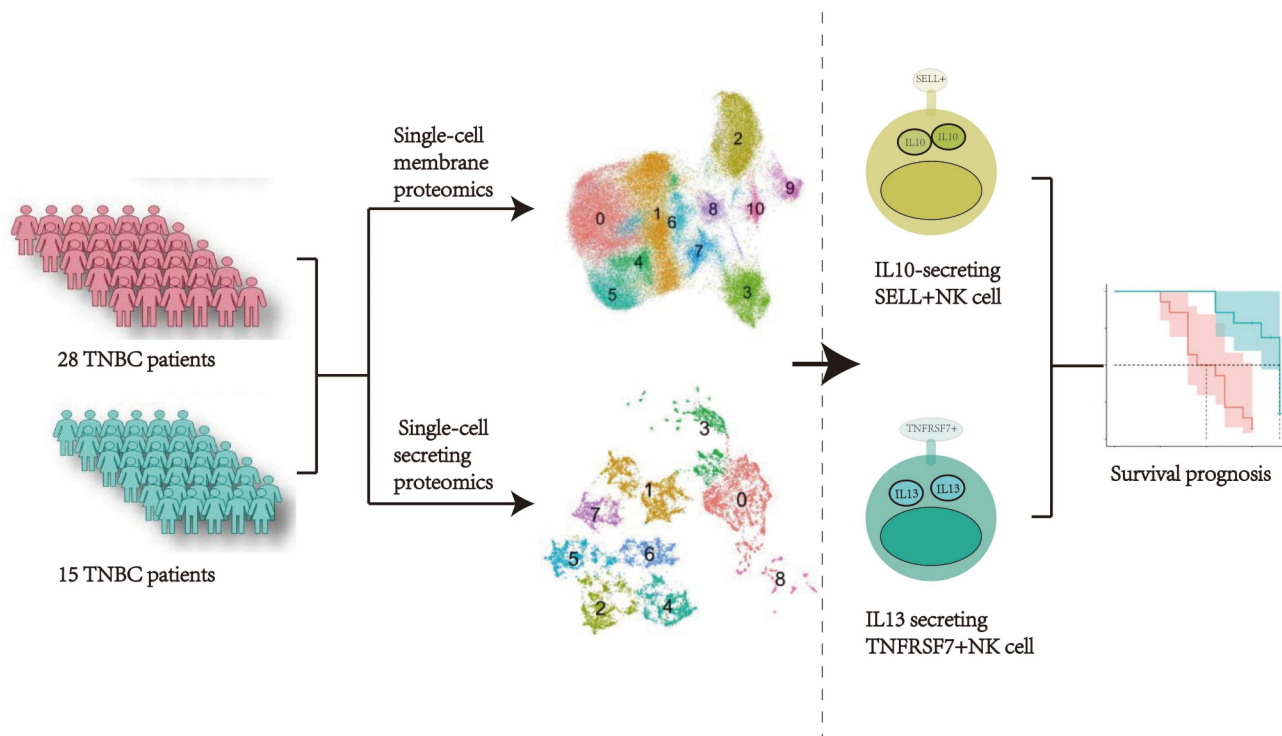


Fig. 4 Schematic figure of proposed model of how the different NK cell populations relate to PFS

High levels of IL10 were associated in prior research with escape from immune attack and poor outcomes [20]. While TNFRSF7 + TINKs secreted IL13, a cytokine traditionally linked to Th2-mediated immune activation, IL13 has dual roles in cancer. It may promote tumor growth by inducing fibroblast activation and extracellular matrix remodeling [21]. On the other hand, it may suppress anti-tumor immunity via macrophage polarization, leading to an immunosuppressive tumor microenvironment that supports tumor growth [22]. Further research is needed to clarify how IL-13 from TNFRSF7 + TINKs balances these effects in TNBC. Further research may involve modulating functions of SELL + NK cells, especially moderating IL secretion or targeting TNFRSF7 to achieve better immune activation.

In addition, prior studies of neoadjuvant chemotherapy in TNBC exhibited that immune activation in the periphery may be associated with high residual disease state [23]. However, in this study, most clusters in the periphery and peritumoral tissues were functionally deficient but were not associated with patient outcomes during our 18-month follow-up, probably due to low statistical power. As such, future research is encouraged to decipher interactions of patient outcomes associated with NK cells from periphery or peritumorous tissue.

Also, single-cell cytokine profiling demonstrated that these cells potentially secrete functional cytokines consistent with cell phenotypes in SELL + and TNFRSF7 + cells. How these two functionally divergent NK subsets

interact within the tumor microenvironment encourages future research to illuminate future therapeutic targets. Furthermore, previous research in the single-cell transcriptomic analysis of pan-cell types of cancer specimens evidenced that NK cell mainly functions as potent immune surveillance [24]. However, our findings in TNBC patients suggested energetic or inhibitory NK cell clusters were the main subtypes specific to either tumor or periphery, featured by loss of typical NK cell receptors, including Nkp30, KLRK1, and FcγRIII. This preliminary finding answered treatment resistance and poor outcomes in TNBC patients, and future mechanistic research is encouraged.

Limitations

There are several limitations in our study. As mentioned, although we procured enough cell counts for phenotype profiling at a single-cell level, the patient number remained low for robust statistical calculation, such as log-rank test. NK cell counts per patient remained relatively low. NK cells were challenging to isolate due to biological rarity, sampling obstacles, and lost cells from single-cell protocols. In addition, membrane or cytokine profiling was limited by antibodies adopted in our study. The panels encompassed 82 membrane proteins and 32 cytokines for analysis at protein levels, but other cytokines or membrane markers are yet to be profiled, limiting sub-cluster identification.

Methods

Human participants and settings

Patients were enrolled for development cohort in the Affiliated Cancer Hospital of Shantou University Medical College and the Hainan Hospital of PLA General Hospital from 2022.4 to 2023.3. In the validation cohort, patients were enrolled in the First Affiliated Hospital of Fujian Medical University from 2023.1 to 2023.9. The human participant study followed Institutional Review Boards at the Cancer Hospital of Shantou University Medical College with approved protocols and required informed consent by all participants of the study. All sampling procedures were performed according to the Helsinki Declaration. Information related to demographic variables and treatment history of participants were obtained from electronic medical records at each research setting as de-identified data. Reporting adhered to Strengthening the Reporting of Observational Studies in Epidemiology (STROBE) checklist for cohort studies.

The primary aim of the research was to profile NK cell sub-clusters in the context of NATI-resistant TNBC, and the secondary aim was to find associations between cell clusters in each patient and follow-up outcomes. Thus, a pathology review was performed to exclude patients with pCR or RCB-I disease, of whom prognosis would have been excellent. Key inclusion criteria were as follows: (a) female patients aged 18 to 60 years; (b) TNBC patients with RCB II/III diagnosis (c) T2 and T3 cancer stage, or N1 to N3 nodal stage, or high grade (grade 3) before NATI. Key exclusion criteria were follow-up data not complete for study endpoint evaluation or volunteered withdrawal from follow-up or the current study. Patients were followed up in outpatient and inpatient services as routine medical checkups. Imaging studies as well as lab tests would be involved if necessary to determine disease progression, defined according to RECIST 1.1 (Response Evaluation Criteria in Solid Tumors). Follow-up was carried out on a 1-3-month basis for half a year after surgery, and on a 3-6-month base afterward until 18 months after surgery in both cohorts. For the current study, we evaluated progression-free survival (PFS) since no patient died at the end of follow-up (as of 2024.9). PFS was calculated from surgery to disease progression or censored to last follow-up, which was defined as the primary endpoint of the clinical research part. Degree of disease was evaluated with RECIST 1.1 according to clinical exams, lab tests, and/or imaging studies of ultrasound, mammography as well as MRI.

Isolation of NK cells from surgery specimen samples

Fresh TNBC samples and para-cancerous samples were collected as surgical specimens from the Department of General Surgery. Samples were minced and incubated into a RPMI-1640 medium (Gibco, #11875093),

including 10% heat-inactivated fetal bovine serum (FBS) (Gibco, #10099141), Normocin (10 µg/ml) (InvivoGen, #ant-nr-1), DNase I (2 µg/ml) (Roche, #4716728001), and collagenase IV (1 mg/ml) (Worthington Biochem, #LS004186). The mix was shaken at 37 °C for 30 min. The cell suspension was then filtered into a 70-µm filter and washed up by RPMI-1640 media. Cells were then resuspended in a 37.5% Percoll density gradient medium (Cytiva, #17-0891-01) and centrifuged (690 g, 25 min, room temperature) to obtain lymphocytes. PBMCs were purified with Ficoll-Paque plus gradient (Cytiva, #17144003) and LeucoSep tubes according to the manufacturer manual (Greiner Bio-One, #227290). Cells were then washed in flow cytometry buffer (PBS with 2% FBS and 2 mM EDTA) at 4 °C and blocked with human Fc Block (1:100, flow cytometry buffer; Miltenyi Biotec, #130-059-901). Viable cells were purified from dead cells with Ficoll-Paque Plus medium (GE Healthcare). Human NK cells were enriched by positive selection with CD56 (NCAM1) microbeads (Miltenyi Biotec, #130-097-042). Human IL-10 ELISA kits were purchased from JinYiBai (Nanjing, China) and were measured according to the manufacturer protocol.

Single-cell membrane proteomics and single-cell secreting proteomics

The aim of single-cell membrane proteomics was to define membranous phenotypes of NK cells isolated from paired samples. As NK cell phenotypes in TNBC has largely been unknown so far, we designed a panel of 82-membrane marker antibody panel using Abseq platform by reference of previous NK cell phenotype research as well as other research adopting high-dimensional analysis [25–27]. Also, considering that CD56 (NCAM1) may encompass most NK lineages and cell isolation challenges in tissue specimen, we adopted CD56+ (NCAM1+) microbeads for NK cell sorting. For secreting proteomics, the primary goal was to profile 32 cytokines at a single-cell level for NK cell subset of interest after analysis of single-cell membrane proteomics.

Isolated cells were labeled with Single-Cell Multiplexing Kit (# 633781, BD Biosciences) as well as BD AbSeq Ab-Oligos for 2 h, following the manufacturer manual, with antibodies shown in Supplementary Table 1. NK cells were isolated and cryopreserved for single-cell secreting proteomics. Cell samples were thawed and cultured in a complete RPMI medium (Fisher Scientific) at a density of 1×10^5 cells/mL, and viable cells were purified as noted above. Cell subclusters of interest (SELL+ NK cells and TNFRSF7+ NK cells in single-cell suspensions of tumor tissue) were isolated with SELL microbeads (#130-091-758, Miltenyi Biotec) as well as TNFRSF7+ microbeads (#130-051-601, Miltenyi Biotec) as positive selection and resuspended in complete RPMI

media. The cell suspension was loaded onto an IsoCode Chip (IsoPlexis) and incubated at 37 °C, 5% CO₂ for 16 to 24 h. Secreted proteins from 1000 to 2000 cells were captured by 32-plex antibody barcoded chip (Supplementary Table 2) and computed with backend fluorescence ELISA-based assay [28, 29].

Single-cell data analysis

Data cleansing and auto-clustering were performed with the “*Seurat*” package on R (version 4.3.1) Statistics. Cells without any barcoded antibody and any antibody covering < 50 cells were excluded from the analysis. Dimension reduction was first carried out with principal component analysis (PCA) and then with Uniform Manifold Approximation and Projection (UMAP) to offer unsupervised auto-clustering of single cells. PCA was carried out using all available protein antibodies for analysis. In single-cell membrane proteomics, 13 components were applied for the UMAP plot in each analysis, with a resolution set as 0.3. In single-cell secreting analysis, 11 components of principle components were applied for the UMAP plot, with a resolution set as 0.1. Default-parameter “FindAllMarkers” embedding was adopted for marker identification in any specific cluster with a 0.25 difference from all other clusters and the threshold for cell proportion was set at 0.25. Global scaling was performed prior to log transformation and centering from counts of barcoded antibodies found by sequencing or illuminant secreting index. Annotation of single-cell membrane proteomics-defined cluster was performed by referencing Cellmarker (version 2.0) [30].

Statistical calculation

Data related to grouping and cell counts were analyzed using non-parametric tests, including Wilcoxon signed-rank test for continuous variables and McNemar test for categorical variables. To calculate associated risk factors of progression-free survival (PFS) rate in the 18-month follow-up, Kaplan-Meier analytic protocols were adopted. Univariate followed by multivariate Cox proportional hazard test was applied for comparison of differences in PFS rate in comparable groups. Cell clusters in each patient were calculated as proportions that entered survival analysis. Patient grouping was delineated by median cell cluster proportions of these patients, and “XX_low” was illustrated as patients with this cluster proportion lower than median. Both single-cell membrane proteomics of NK cells and secreting proteomics were calculated by grouping of median proportion. Then, factors significant in univariate analysis entered multivariate Cox models with an aim to adjust for clinicopathological variables. The hazard ratio (95% confidence interval, CI) was reported for each variable which was visualized as forest plots.

Supplementary Information

The online version contains supplementary material available at <https://doi.org/10.1186/s13058-025-02003-y>.

Supplementary Material 1
Supplementary Material 2
Supplementary Material 3
Supplementary Material 4
Supplementary Material 5
Supplementary Material 6
Supplementary Material 7
Supplementary Material 8

Acknowledgements

The authors would like to acknowledge the volunteers who participated in the study.

Author contributions

Y. M and G. Z conceptualized and designed the study, and reviewed and revised the manuscript. Y. W, J. L, and J. Z designed the data collection instruments, carried out the initial analyses, and wrote the first draft of the manuscript. Y. J, T. H, Y. M, J. L, X. W, H. Y, X. L, Y. N, coordinated and supervised data collection and critically reviewed the manuscript for important intellectual content. F. D, P. Z, J. L, W. W, X. Q, J. L, B. C, T. H collected data and reviewed and revised the manuscript. All authors approved the final manuscript as submitted and agreed to be accountable for all aspects of the work. The work reported in the paper has been performed by the authors unless specified in the text.

Funding

This work was supported by the Joint Funds for the Innovation of Science and Technology, Fujian Province (No.2023Y9054 to Y.M); Guangdong Basic and Applied Basic Research Foundation Key Project (No.2023B1515230004 to X.W); and Science and Technology Special Fund of Guangdong Province of China (STKJ2023002 to X.W) (Note: All the funders had no role in the design and conduct of the study.)

Data availability

Data are available on reasonable request.

Declarations

Ethics approval and consent to participate

The study was approved for retrospective protocol by the institutional review boards of the First Affiliated Hospital of Fujian Medical University. All procedure was performed according to the Helsinki Declaration.

Consent for publication

Participants had given written informed consent to the usage of clinical information for medical research.

Competing interests

The authors declare no competing interests.

Author details

¹Department of General Surgery, Hainan Hospital of People's Liberation Army General Hospital, Sanya, Hainan, China

²Department of Nuclear Medicine, State Key Laboratory of Oncology in South China, Collaborative Innovation Center for Cancer Medicine, Sun Yat-sen University Cancer Center, Guangzhou, Guangdong, China

³State Key Laboratory of Oncology in South China, Guangdong Key Laboratory of Nasopharyngeal Carcinoma Diagnosis and Therapy, Guangdong Provincial Clinical Research Center for Cancer, Sun Yat-sen University Cancer Center, Guangzhou, Guangdong, China

⁴Department of Hepatobiliary and Pancreatic Surgery, The First Affiliated Hospital of Fujian Medical University, Fuzhou, Fujian, China

⁵Fujian Provincial Key Laboratory of Precision Medicine for Cancer, The First Affiliated Hospital of Fujian Medical University, Fuzhou, Fujian, China

⁶Institute of Abdominal Surgery, The First Affiliated Hospital of Fujian Medical University, Fuzhou, Fujian, China

⁷Department of Hepatobiliary and Pancreatic Surgery, National Regional Medical Center Binhai Campus of the First Affiliated Hospital, Fujian Medical University, Fuzhou, Fujian, China

⁸Department of Hepatobiliary Surgery, The First Affiliated Hospital of Shantou University Medical College, Shantou, Guangdong, China

⁹Department of General Surgery, General Hospital of XinJiang Military Command, Urumqi, XinJiang, China

¹⁰Department of Clinical Laboratory, State Key Laboratory of Oncology in South China, Collaborative Innovation Center for Cancer Medicine, Guangdong Key Laboratory of Nasopharyngeal Carcinoma Diagnosis and Therapy, Sun Yat-sen University Cancer Center, Guangzhou, Guangdong, China

¹¹Department of Clinical Laboratory & Key Clinical Laboratory of Henan province, The First Affiliated Hospital of Zhengzhou University, Zhengzhou, Henan, China

¹²Department of Laboratory Medicine, Taiyuan Central Hospital of Shanxi Medical University, Taiyuan, Shanxi, China

¹³Department of Anesthesiology, Tongji Shanxi Hospital, Shanxi Bethune Hospital, Shanxi Academy of Medical Sciences, Third Hospital of Shanxi Medical University, Taiyuan, Shanxi, China

¹⁴Department of Orthopedics and Spine Surgery, The Second Affiliated Hospital of Shantou University Medical College, Shantou, Guangdong, China

¹⁵Department of Orthopedics and Spine Surgery, Cancer Hospital of Shantou University Medical College, Shantou, Guangdong, China

¹⁶Department of Neurology, Hainan Hospital of Chinese PLA General Hospital, Sanya, Hainan, China

¹⁷XLifeSc, Ltd, Guangzhou, Guangdong, China

¹⁸Department of Clinical Laboratory Medicine, Cancer Hospital of Shantou University Medical College, Shantou, Guangdong, China

¹⁹Internal Medicine Department, Jacobi Medical Center, 1400 Pelham Play S, Bronx, NY, USA

²⁰Acute Communicable Disease Epidemiology Division, Dallas County Health and Human Services, Dallas, TX, USA

²¹Department of Gastroenterology, Hainan Hospital of Chinese PLA General Hospital, Sanya, Hainan, China

²²Key Laboratory of Biochemistry and Molecular Biology, Hainan Medical University, Haikou, Hainan, China

²³Department of thoracic surgery, The First People's Hospital of Shangqiu City Affiliated to Xinxiang Medical University, Shangqiu, Henan, China

Received: 10 December 2024 / Accepted: 15 March 2025

Published online: 03 April 2025

References

- Li Y, Jiang-Jie D, Xiu-Wu B, Shi-Cang Y. Triple-negative breast cancer molecular subtyping and treatment progress. *Breast Cancer Res.* 2020;22(1). <https://doi.org/10.1186/s13058-020-01296-5>
- Licià R, Chiara C, Giovanni F, et al. Immunological characterization of a long-lasting response in a patient with metastatic triple-negative breast cancer treated with PD-1 and LAG-3 blockade. *Sci Rep.* 2024;14(1). <https://doi.org/10.1038/s41598-024-54041-9>
- Tanya EK, Sara MT. Role of immunotherapy in triple-negative breast cancer. *J Natl Compr Canc Netw.* 2020;18(4). <https://doi.org/10.6004/jnccn.2020.7554>
- Patrycja G, Charlotte M, Jacopo I, et al. Dynamic changes in the NK-, neutrophil-, and B-cell immunophenotypes relevant in high metastatic risk post neoadjuvant chemotherapy-resistant early breast cancers. *Clin Cancer Res.* 2022;28(20). <https://doi.org/10.1158/1078-0432.ccr-22-0543>
- Heran D, Liying W, Na W, et al. Neoadjuvant checkpoint blockade in combination with chemotherapy in patients with triple-negative breast cancer: exploratory analysis of real-world, multicenter data. *BMC Cancer.* 2023;23(1). <https://doi.org/10.1186/s12885-023-10515-z>
- María Rosario C-P, Ana G-O, Begoña J, Nuria R, Isabel B, Emilio A. Resistance to neoadjuvant treatment in breast cancer: clinicopathological and molecular predictors. *Cancers (Basel).* 2020;12(8). <https://doi.org/10.3390/cancers12082012>
- Fernando S-F-G, Joseph C, Nicholas DH. The emergence of natural killer cells as a major target in cancer immunotherapy. *Trends Immunol.* 2019;40(2). <http://doi.org/10.1016/j.it.2018.12.003>
- Joshua KMW, Riccardo D, Handoo R, Fiona S, Fernando S, -F-G. Weaponizing natural killer cells for solid cancer immunotherapy. *Trends Cancer.* 2022;9(2). <https://doi.org/10.1016/j.trecan.2022.10.009>
- Laurence Z, Lionel A, François G, Guido K. Immunological aspects of cancer chemotherapy. *Nat Rev Immunol.* 2007;8(1). <https://doi.org/10.1038/nri2216>
- Song-Yang W, Tong F, Yi-Zhou J, Zhi-Ming S. Natural killer cells in cancer biology and therapy. *Mol Cancer.* 2020;19(1). <https://doi.org/10.1186/s12943-020-01238-x>
- Yuanshuo AW, Daniel R, Christine B, et al. NK cell-targeted immunotherapies in bladder cancer: beyond checkpoint inhibitors. *Bladder Cancer.* 2024;9(2). <https://doi.org/10.3233/blc-220109>
- Beatriz S-C, Nelson L-S, Esther D, et al. Modulation of NK cells with checkpoint inhibitors in the context of cancer immunotherapy. *Cancer Immunol Immunother.* 2019;68(5). <https://doi.org/10.1007/s00262-019-02336-6>
- Joshua KMW, Timothy RM, Louisa A, et al. TGF- β signalling limits effector function capacity of NK cell anti-tumour immunity in human bladder cancer. *EBioMedicine.* 2024;104(0). <https://doi.org/10.1016/j.ebiom.2024.105176>
- Emilie M, Aude S, François B, et al. Human breast tumor cells induce self-tolerance mechanisms to avoid NKG2D-mediated and DNAM-mediated NK cell recognition. *Cancer Res.* 2011;71(21). <https://doi.org/10.1158/0008-5472.can-11-0792>
- Yansong L, Mingcui L, Zhengbo F, et al. Overexpressing S100A9 ameliorates NK cell dysfunction in estrogen receptor-positive breast cancer. *Cancer Immunol Immunother.* 2024;73(7). <https://doi.org/10.1007/s00262-024-0369-9-1>
- Chandan V, Viriya K, Jennifer ME, et al. Natural killer (NK) cell profiles in blood and tumour in women with large and locally advanced breast cancer (LLABC) and their contribution to a pathological complete response (PCR) in the tumour following neoadjuvant chemotherapy (NAC): differential restoration of blood profiles by NAC and surgery. *J Transl Med.* 2015;13(0). <https://doi.org/10.1186/s12967-015-0535-8>
- Iñaki E, Javier G-V, Álvaro T, Ignacio M. New emerging targets in cancer immunotherapy: CD137/4-1BB costimulatory axis. *ESMO Open.* 2020;4(0). <https://doi.org/10.1136/esmoopen-2020-000733>
- Hui S, Yuzhang W, Yi Z, Bing N. IL-10-producing ILCs: molecular mechanisms and disease relevance. *Front Immunol.* 2021;12(0). <https://doi.org/10.3389/fimmu.2021.650200>
- Norberto WZ, Carolina ID, Mercedes BF. Regulatory functions of NK cells during infections and cancer. *J Leukoc Biol.* 2020;109(1). <https://doi.org/10.1002/jlb.3mr0820-685r>
- Yekaterina OO, Esin Aktas C, Yuliya VP, et al. Peripheral blood NK cells expressing HLA-G, IL-10 and TGF- β in healthy donors and breast cancer patients. *Cell Immunol.* 2015;298(0). <https://doi.org/10.1016/j.cellimm.2015.09.002>
- Little A, Pathanjeli P, Wu Z, et al. IL-4/IL-13 stimulated macrophages enhance breast cancer invasion via Rho-GTPase regulation of synergistic VEGF/CCL-18 signaling. *Front Oncol.* 2019;9:456. <https://doi.org/10.3389/fonc.2019.00456>
- Ito A, Akama Y, Satoh-Takayama N, et al. Possible metastatic stage-dependent ILC2 activation induces differential functions of MDSCs through IL-13/IL-13R α 1 signaling during the progression of breast cancer lung metastasis. *Cancers.* 2022;14(13). <https://doi.org/10.3390/cancers14133267>
- Margaret LA, Mellissa JN, Paula I, G-E, et al. Changes in peripheral and local tumor immunity after neoadjuvant chemotherapy reshape clinical outcomes in patients with breast cancer. *Clin Cancer Res.* 2020;26(21). <https://doi.org/10.1158/1078-0432.ccr-19-3685>
- Le T, Carlos J-C, Apple HMT, Stina W, Lorenzo G, Andreas L. NK cells and solid tumors: therapeutic potential and persisting obstacles. *Mol Cancer.* 2022;21(1). <https://doi.org/10.1186/s12943-022-01672-z>
- Alvaro H-I, Marianna V, Herman N, et al. Adaptive single-KIR(+)NKG2C(+) NK cells expanded from select superdonors show potent missing-self reactivity and efficiently control HLA-mismatched acute myeloid leukemia. *J Immunother Cancer.* 2022;10(11). <https://doi.org/10.1136/jitc-2022-005577>
- Ila D, Miguel FS, Jun W, et al. Expression analysis and significance of PD-1, LAG-3, and TIM-3 in human non-small cell lung cancer using spatially resolved and multiparametric single-cell analysis. *Clin Cancer Res.* 2019;25(15). <https://doi.org/10.1158/1078-0432.ccr-18-4142>
- Priyanka BS, Zhiwan D, Daniel G, et al. Distinct predictive biomarker candidates for response to anti-CTLA-4 and anti-PD-1 immunotherapy in

- melanoma patients. *J Immunother Cancer*. 2018;6(1). <https://doi.org/10.1186/s40425-018-0328-8>
28. Dong L, Patrick P, Sean M, Colin N, Jing Z. Single-cell multiplexed proteomics on the IsoLight resolves cellular functional heterogeneity to reveal clinical responses of cancer patients to immunotherapies. *Methods Mol Biol*. 2019;2055(0). https://doi.org/10.1007/978-1-4939-9773-2_19
29. Hussein AA, Zoe A, Sean M, et al. Single-cell polyfunctional proteomics of CD4 cells from patients with AML predicts responses to anti-PD-1-based therapy. *Blood Adv*. 2021;5(22). <https://doi.org/10.1182/bloodadvances.2021004583>
30. Congxue H, Tengyue L, Yingqi X, et al. CellMarker 2.0: an updated database of manually curated cell markers in human/mouse and web tools based on scRNA-seq data. *Nucleic Acids Res*. 2022;51(0). <https://doi.org/10.1093/nar/gkac947>

Publisher's note

Springer Nature remains neutral with regard to jurisdictional claims in published maps and institutional affiliations.